AIP | Applied Physics Letters

Room temperature continuous-wave operation of In As/In P (100) quantum dot lasers grown by gas-source molecular-beam epitaxy

S. G. Li, Q. Gong, Y. F. Lao, K. He, J. Li, Y. G. Zhang, S. L. Feng, and H. L. Wang

Citation: Applied Physics Letters **93**, 111109 (2008); doi: 10.1063/1.2985900
View online: http://dx.doi.org/10.1063/1.2985900
View Table of Contents: http://scitation.aip.org/content/aip/journal/apl/93/11?ver=pdfcov
Published by the AIP Publishing

Room temperature continuous-wave operation of InAs/InP(100) quantum dot lasers grown by gas-source molecular-beam epitaxy

S. G. Li,[1] Q. Gong,[1,a)] Y. F. Lao,[1] K. He,[1] J. Li,[1] Y. G. Zhang,[1] S. L. Feng,[1] and H. L. Wang[2]
[1]*State Key Laboratory of Functional Materials for Informatics, Shanghai Institute of Microsystem and Information Technology, Chinese Academy of Sciences, 865 Changning Road, Shanghai 200050, People's Republic of China*
[2]*College of Physics and Engineering, Qufu Normal University, Qufu 273165, People's Republic of China*

(Received 22 July 2008; accepted 28 August 2008; published online 18 September 2008)

We report on the InAs quantum dots (QDs) laser in the 1.55 μm wavelength region grown by gas source molecular-beam epitaxy. The active region of the laser structure consists of fivefold-stacked InAs QD layers embedded in the InGaAsP layer. Ridge waveguide lasers were processed and continuous-wave mode operation was achieved between 20 and 70 °C, with characteristic temperature of 69 K. High internal quantum efficiency (56%) and low infinite length threshold current density (128 A/cm^2 per QD layer) was obtained for the as-cleaved devices at room temperature. The lasing wavelength range between 1.556 and 1.605 μm can be covered by varying the laser cavity length. © *2008 American Institute of Physics*. [DOI: 10.1063/1.2985900]

InAs quantum dots (QDs) on GaAs or InP substrates are very promising active materials for lasers[1] and semiconductor optical amplifiers[2] used in fiber optical telecommunication systems, provided their emission wavelength is within the 1.31 or 1.55 μm regions. In order to match these two telecommunication wavelength windows, much effort has been respectively devoted to achieving InAs/GaAs QDs emitted at 1.31 μm,[3,4] and InAs/InP QDs at 1.55 μm.[5–8] In particular, for InAs/InP QDs, three methods have been reported to obtain the desired emission wavelength, i.e., (1) postgrowth annealing the InAs QDs on InP substrates,[5] (2) applying ultrathin GaAs or GaP interlayers between InAs QD layer and the buffer layer,[6,7,9] and (3) formation of QDs by (In,Ga)As layers with very low Ga composition instead of pure InAs layer.[8] Most studies have been carried out on metal-organic vapor-phase epitaxy[8,9] (MOVPE) and chemical-beam epitaxy.[6,7] Recently, Lelarge *et al.*[10] reported buried ridge stripe lasers with InAs/InP(100) QDs as the active core by gas-source molecular-beam epitaxy (GSMBE), operating at 1.46–1.5 μm in continuous-wave (cw) mode, without utilization of any particular procedure mentioned above during the growth of InAs QDs but adjusting the thickness of deposited InAs layer. However, a large blueshift of 80 nm was observed due to In–Ga and As–P intermixing during the high temperature MOVPE regrowth of P-doped InP cladding and (In,Ga)As contact layers.[10] The thermally enhanced intermixing is undesirable, which leads to lasing wavelength much shorter than 1.55 μm. In this letter, we report on the 1.55 μm InAs/InP(100) QD lasers with all layers in the laser structure grown by GSMBE. The as-cleaved ridge waveguide lasers operated in cw mode up to 70 °C, with characteristic temperature of 69 K between 20 and 70 °C and the maximum output power is more than 30 mW from one facet at room temperature. The dependence of threshold current density on cavity length reveals very low infinite length threshold current density of 638 A/cm^2, i.e., 128 A/cm^2 per QD layer.

The samples were grown on nominally (100) exact oriented *n*-type InP substrates by GSMBE using gallium and indium as sources of III element. On the other hand, the V element sources are obtained by introducing AsH_3 and/or PH_3 through the high temperature injector where the gases are thermally decomposed at 1000 °C. The QD lasers included fivefold-stacked InAs QD layers separated by 40-nm-thick InGaAsP barriers (λ_g=1.18 μm) as the active core, which was embedded in a 200-nm-thick InGaAsP layer (λ_g=1.18 μm) for separate confinement. The bottom and top cladding layers are 600 nm *n*-InP buffer and 1.5 μm *p*-InP followed by 200 nm *p*-InGaAs contact layer. Each QD layer was formed by deposition of 3.0 ML InAs at 485 °C with InAs growth rate of 0.1 ML/s, while the AsH_3 pressure in the gas line was set as 630 Torr and the growth chamber pressure was measured as 1.5×10^{-5} Torr during the QD growth. In order to achieve the desirable emission wavelength, the layer thickness of InAs was chosen as 3.0 ML. The surface morphology of a single QD layer grown on the InGaAsP barrier was measured by atomic force microscopy (AFM), revealing the formation of QD with high density in the 10^{10} cm^{-2} range, as shown in Fig. 1(a). The well defined QDs were found to be slightly elongated along the $[01\bar{1}]$ direction with mean dot height of 2.9 nm and mean base

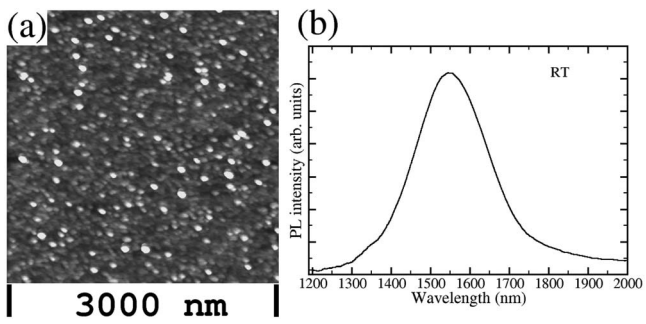

FIG. 1. (a) AFM image of the InAs QDs on InGaAsP lattice matched to InP(100) formed by depositing 3.0 ML InAs. The black-to-white height contrast is 10 nm. (b) PL spectrum taken at room temperature of the InAs QDs embedded in InGaAsP.

a)Author to whom correspondence should be addressed. Electronic mail: qgong@mail.sim.ac.cn.

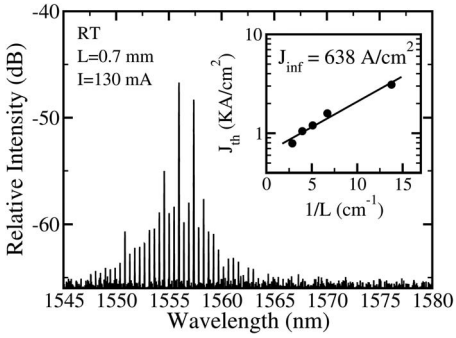

FIG. 2. Lasing spectrum at room temperature of the QD laser with 0.7 mm long cavity length, under cw injection current of 130 mA, i.e., 1.02× threshold current. Inset is the threshold current density as a function of reciprocal cavity length $(1/L)$, measured at room temperature in cw mode.

diameter of 76 nm. Room temperature photoluminescence (PL) spectrum of the InAs QDs embedded in InGaAsP layer was shown in Fig. 1(b), with linewidth of about 108 meV. Ridge waveguide QD lasers with stripe width of 6 μm and different cavity lengths were processed, leaving as-cleaved laser facets. Device performance characterization were carried out between 20–85 °C in cw operation mode. The lasing spectra were measured by an optical spectrum analyzer with wavelength resolution of 0.01 nm, through an single mode fiber located close to the laser facet. The output power measurements were performed by a Melles Griot optical power meter equipped with a integrating sphere Ge detector.

Multimode laser spectrum centered at 1.556 μm was measured from the QD laser with cavity length of 0.7 mm and stripe width of 6 μm, as shown in Fig. 2, where the injected current of 130 mA is just above the threshold current (128 mA). The threshold current density J_{th} is found to drop from 3.1 kA/cm^2 to 790 A/cm^2 with the increase in cavity length from 0.7 to 3.5 mm, as shown in the inset of Fig. 2. From the dependence of J_{th} on cavity length, i.e., $\ln(J_{th}) \propto 1/L$, a threshold current density for infinite cavity length was derived as low as 638 A/cm^2, which corresponds to about 128 A/cm^2 per QD layer.

Figure 3 shows the light output characteristics of the QD laser with cavity length of 2 mm, under cw operation with heat sink temperature ranging from 20 to 70 °C. At 20 °C, the QD laser has threshold current of 1.1 kA/cm^2, and maximum output power above 30 mW/facet, with slope efficiency of 94 mW/A just above the threshold. The maximum output power drops gradually to about 5 mW when the heat sink

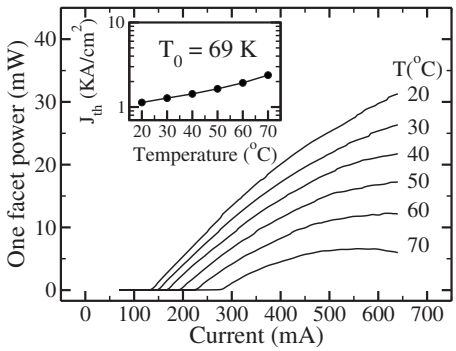

FIG. 3. Output power vs injection current of a 2-mm– long as-cleaved QD laser under cw operation in the temperature range of 20–70 °C. Inset is the threshold current density versus temperature.

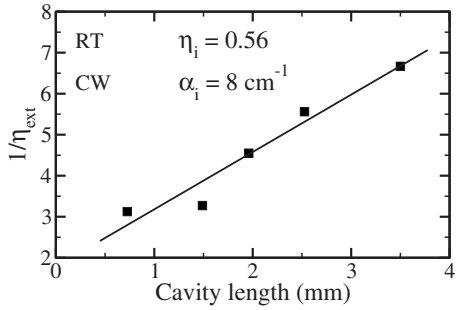

FIG. 4. Dependence of reciprocal external differential efficiency on cavity length of the InAs QD lasers.

temperature is raised to 70 °C. The laser threshold current density as a function of operation temperature is shown in the inset of Fig. 3. Characteristic temperature of 69 K is derived in the temperature range 20–70 °C, by equation $J_{th}(T)=J_0 \exp(T/T_0)$. It is higher than those values previously reported, i.e., 25 K (20–30 °C) (Ref. 9) and 56 K (20–80 °C).[10] In detail, two different slopes appear in the inset of Fig. 3, corresponding to characteristic temperatures of 81 K (20–50 °C) and 54 K (50–70 °C) respectively, likely due to the existence of thermally activated nonradiative process.[11]

Figure 4 shows the reciprocal external differential efficiency as a function of the cavity length. The internal optical loss and quantum efficiency can be derived from the dependence of measured external quantum efficiency on the cavity length by the following equations:

$$\eta_{\text{ext}} = \frac{2q}{h\nu}\frac{dP}{dI}, \tag{1}$$

$$\frac{1}{\eta_{\text{ext}}} = \frac{1}{\eta_i}\left(1 + \frac{\alpha_i L}{\ln\frac{1}{R}}\right), \tag{2}$$

where η_{ext} is the external differential efficiency, η_i is the internal quantum efficiency, q is the electronic charge, h is the Plank constant, ν is the optical frequency, P is the output power from a single facet, I is the injection current, L is the cavity length, α_i is the internal loss, and R is reflectivity of the cleaved facet. The derived internal optical loss and the internal quantum efficiency is 8 cm^{-1} and 56%, respectively, taking the facet reflectivity as 0.35. Compared to the 1.55 μm wavelength InAsP/InGaAsP strained multi-quantum-well lasers,[12] the internal quantum efficiency of InAs/InP QD laser is still low. However, it is expected to drastically improve the internal quantum efficiency by optimizing the growth conditions of InAs QDs for better QD size uniformity. In comparison with the InAs/GaAs QD assembly, the InAs/InGaAsP/InP(100) QD assembly has very large size distribution, indicated by the very broad PL peak, e.g., linewidth of about 108 meV at room temperature measured by us and reported by other groups.[9,10]

One interesting feature of the InAs/InGaAsP/InP QD laser is the cavity length dependence of the lasing wavelength, which decreases from 1.605 to 1.556 μm with the reduction of cavity length from 3.5 to 0.7 mm, as shown in Fig. 5(b). The lasing spectra centered at 1.556 and 1.594 μm of two devices are shown in Fig. 5(a), with cavity length of 0.7 and 2 mm, respectively. The wavelength difference of the

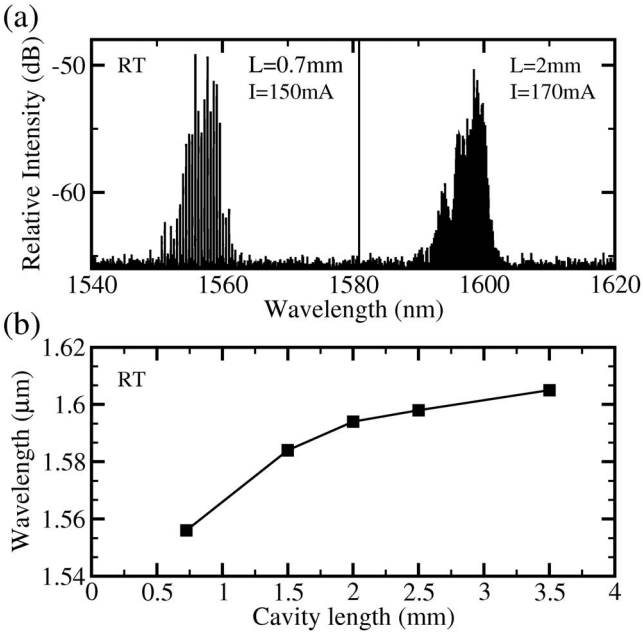

FIG. 5. (a) Lasing spectrum taken at room temperature in cw operation mode for QD lasers with cavity length of 0.7 and 2.0 mm, respectively. (b) Lasing wavelength vs cavity length varying from 0.7 to 3.5 mm.

two laser peaks shown in Fig. 5(a) corresponds to an energy separation of about 19 meV, which is much less than what is between the ground-state (GS) transition in small QDs and large QDs, revealed by the broad PL peak of QD assembly at room temperature with width of about 108 meV. The broad size distribution of the QD assembly leads to a broad gain spectrum of the QD laser. In addition, the bigger InAs/InP(100) QDs than InAs/GaAs ones result in much smaller ground-state/excited-state (ES) splitting for InAs/InP QDs, e.g., 31 meV for InAs/InP(311)B QDs.[11] In contrast, the InAs/GaAs QDs have GS-ES splitting more than 90 meV.[13] Thus, the gain spectrum in the lasing wavelength range may include contributions from both GS transitions and ES transitions of the QD assembly. The mirror loss rises with decrease in the cavity length, leading to shorter operating wavelength where the laser diode can provide enough gain for lasing.

In summary, InAs/InGaAsP/InP(100) QD lasers operating in the 1.55 μm wavelength region have been grown by GSMBE, with the active region including fivefold-stacked QD layers. CW operation of the QD lasers have been achieved at temperatures up to 70 °C. The characteristic temperature of the QD lasers was obtained as 69 K between 20 and 70 °C. From the measured dependence of laser characteristics on the cavity length at room temperature, we derived the internal quantum efficiency as high as 56%, internal optical loss of 8 cm^{-1}, and the threshold current density for infinite cavity length of 638 A/cm^2, i.e., 128 A/cm^2 per QD layer.

The authors gratefully acknowledge Dr. C. Lin and Dr. B. Chen for fruitful discussions. This work is supported by the Hundred Talents Program from the Chinese Academy of Sciences, the Shanghai PuJiang Program (Grant No. 06PJ14109), and the National Natural Science Foundation of China (Grant No. 60721004).

[1] D. L. Huffaker, G. Park, Z. Zou, O. B. Shchekin, and D. G. Deppe, Appl. Phys. Lett. **73**, 2564 (1998).
[2] T. Akiyama, N. Hatori, Y. Nakata, H. Ebe, and M. Sugawara, Electron. Lett. **38**, 1139 (2002).
[3] R. P. Mirin, J. P. Ibbetson, K. Nishi, A. C. Gossard, and J. E. Bowers, Appl. Phys. Lett. **67**, 3795 (1995).
[4] V. M. Ustinov, N. A. Maleev, A. E. Zhukov, A. R. Kovsh, A. Yu. Egorov, A. V. Lunev, B. V. Volovik, I. L. Krestnikov, Y. G. Musikhin, N. A. Bert, P. S. Kopev, Zh. I. Alferov, N. N. Ledentsov, and D. Bimberg, Appl. Phys. Lett. **74**, 2815 (1999).
[5] C. Paranthoen, N. Bertru, O. Dehaese, A. Le Corre, S. Loualiche, B. Lambert, and G. Patriarche, Appl. Phys. Lett. **78**, 1751 (2001).
[6] Q. Gong, R. Nötzel, P. J. van Veldhoven, T. J. Eijkemans, and J. H. Wolter, Appl. Phys. Lett. **84**, 275 (2004).
[7] Q. Gong, R. Nötzel, P. J. van Veldhoven, T. J. Eijkemans, and J. H. Wolter, Appl. Phys. Lett. **85**, 1404 (2004).
[8] J. W. Jang, S. H. Ryun, S. H. Lee, I. C. Lee, W. G. Jeong, R. Stevenson, P. Daniel Dapkus, N. J. Kim, M. S. Hwang, and D. Lee, Appl. Phys. Lett. **85**, 3675 (2004).
[9] S. Anantathanasarn, R. Nötzel, P. J. van Veldhoven, F. W. M. van Otten, Y. Barbarin, G. Servanton, T. de Vries, E. Smalbrugge, E. J. Geluk, T. J. Eijkemans, E. A. J. M. Bente, Y. S. Oei, M. K. Smit, and J. H. Wolter, Appl. Phys. Lett. **89**, 073115 (2006).
[10] F. Lelarge, B. Rousseau, B. Dagens, F. Poingt, F. Pommereau, and A. Accard, IEEE Photonics Technol. Lett. **17**, 1369 (2005).
[11] H. Saito, K. Nishi, and S. Sugou, Appl. Phys. Lett. **78**, 267 (2001).
[12] J. F. Carlin, A. V. Syrbu, C. A. Berseth, J. Behrend, A. Rudra, and E. Kapon, Appl. Phys. Lett. **71**, 13 (1997).
[13] H. Shoji, Y. Nakata, K. Mukai, Y. Sugiyama, M. Sugawara, N. Yokoyama, and H. Ishikawa, IEEE J. Sel. Top. Quantum Electron. **3**, 188 (1997).